Carbohydrate Polymers 91 (2013) 100–109

Contents lists available at SciVerse ScienceDirect

Carbohydrate Polymers

journal homepage: www.elsevier.com/locate/carbpol

κ-Carrageenan hydrogel nanocomposites with release behavior mediated by morphological distinct Au nanofillers

Ana M. Salgueiro, Ana L. Daniel-da-Silva*, Sara Fateixa, Tito Trindade

Department of Chemistry, CICECO, University of Aveiro, 3810-193 Aveiro, Portugal

ARTICLE INFO

Article history:
Received 12 April 2012
Accepted 1 August 2012
Available online 8 August 2012

Keywords:
Carrageenan
Hydrogels
Gold nanoparticles
Nanorods
Swelling
Drug release

ABSTRACT

In this work we investigate the effect of spherical and rod-shaped Au nanoparticles (NPs) in the microstructure, thermomechanical and release properties of thermosensitive κ-carrageenan hydrogels. Thermal and mechanical analyses of the composites revealed that the Au NPs reinforce the structure of the hydrogel and the mechanism of gel reinforcement is discussed. The effect of the NPs on the microstructure and strength of the hydrogel had implications in the mechanism of controlled release as demonstrated by *in vitro* release studies using a drug model (methylene blue: MB). Noteworthy, the mechanism of MB release followed either a diffusion or polymer relaxation mechanism, depending on the morphology of the Au NPs incorporated in the hydrogel. Consequently, κ-carrageenan hydrogels containing Au NPs exhibited not only optical features modulated by the fillers morphology, but also showed a behavior as drug carriers that can be also adjusted by Au NPs characteristics.

1. Introduction

Hydrogels derived from natural occurring polysaccharides are high-water content polymeric materials that possess a number of characteristics (*e.g.* high hydrophilicity, biocompatibility, available reactive site for biofunctionalization) favorable for biomedical applications such as drug delivery (Bhattarai, Gunn, & Zhang, 2010; Jain, Gupta, & Jain, 2007; Trindade & Daniel-da-Silva, 2011). The incorporation of inorganic nanoparticles imparts novel functionalities to the hydrogels and is an emerging strategy to design functional materials for multi-task applications, including imaging, sensing and diagnostic in addition to drug delivery (Satarkar, Biswal, & Hilt, 2010; Timko, Dvir, & Kohane, 2010; Trindade & Daniel-da-Silva, 2011).

The introduction of gold nanoparticles (NPs) into hydrogels results in materials with light responsiveness (Choi et al., 2011; Guo et al., 2010; Matteini et al., 2010) which is a valuable property for specific bio-applications. For example, gold chitosan and alginate nanocomposites have shown good results as glucose sensing platforms (Du, Luo, Xu, & Chen, 2007; Lim, Lee, & Park, 2010) while chitosan/Au nanocomposites have been investigated for applications as light activated bioadhesives (Matteini et al., 2010) and drug release nanocarriers (Choi et al., 2011; Guo et al., 2010). The optical features of the nanocomposites are due to the surface plasmon resonance (SPR) effect of Au NPs. The SPR band is sensitive to several parameters including the size and shape of Au NPs (Sharma, Park, & Srinivasarao, 2009). Although nanospheres (NSs) of Au show the SPR in the visible, for some therapeutic applications it is convenient to shift the optical absorption into the near-infrared (NIR) window where absorption of body tissues is minimal. This can be achieved by using anisotropic nanoparticles such as Au nanorods (NRs) instead of nanospheres. The fine tuning of the Au NRs aspect ratio allows the shift of the SPR band of the longitudinal mode to the NIR spectral region. As a result of this optical control the interest in Au NRs for several bio-applications has increased (Stone, Jackson, & Wright, 2011).

Carrageenan comprises a family of linear water-soluble sulfated polysaccharides extracted from red seaweeds. Due to their biocompatibility and ability to form thermoreversible hydrogels, carrageenan has been extensively used as gelling agent in food and pharmaceutical industries (Stephen, Philips, & Williams, 1995). Within the carrageenan family, κ-carrageenan originates the strongest gels and, hence, in the last decade this biopolymer has been investigated as a carrier for controlled drug release (Daniel-da-Silva, Ferreira, Gil, & Trindade, 2011; Daniel-da-Silva et al., 2012; Keppeler, Ellis, & Jacquier, 2009; Leong et al., 2011; Santo et al., 2009). Our recent studies on κ-carrageenan/Fe_3O_4 nanocomposites have revealed that the addition of Fe_3O_4 NPs as nanofillers not only confers magnetic properties to the resulting nanocomposites (Daniel-da-Silva et al., 2007), but can also be used for tailoring the release profile of encapsulated molecules (Daniel-da-Silva et al., 2012).

To the best of our knowledge, the use of κ-carrageenan for preparing optically active carriers upon the incorporation of Au

* Corresponding author. Tel.: +351 234 370 368; fax: +351 234 370 084.
E-mail address: ana.luisa@ua.pt (A.L. Daniel-da-Silva).

0144-8617/$ – see front matter © 2012 Elsevier Ltd. All rights reserved.
http://dx.doi.org/10.1016/j.carbpol.2012.08.004

NPs is an unexplored strategy. Moreover, the effect of Au NPs with variable morphology upon the thermomechanical properties of the hydrogels has not been reported, despite its relevance for drug release applications.

In this work we investigate the role of Au NPs with variable shape (spherical and rod-shaped) on the microstructure, gel strength and release properties of κ-carrageenan hydrogels. Selected hydrogel nanocomposites were tested for the release of methylene blue as drug model in *in vitro* physiological conditions to assess the effect of the nanophases on the kinetics and release mechanism. These systems, due to their optical features, are of particular interest because remotely controlled light triggered drug release may be envisaged, which is an advantage for non-invasive clinical applications.

2. Materials and methods

2.1. Materials

κ-Carrageenan (300.000 g/mol Fluka Chemie), potassium chloride (KCl) (>99%, Sigma–Aldrich), phosphate buffered saline (PBS) (pH 7.4, Sigma–Aldrich), sodium azide (NaN_3) (99%, Sigma–Aldrich), hexadecyltrimethylammoniumbromide (CTAB, 98%, Sigma–Aldrich), benzyldimethylammoniumchloride (BDAC, 98%, Sigma–Aldrich), L-ascorbic acid (Sigma–Aldrich), tetrachloroauric acid ($HAuCl_4{\cdot}3H_2O$) (99.9%, Sigma–Aldrich), trisodium citrate dihydrated ($HOC(COONa)(CH_2COONa)_2{\cdot}2H_2O$) (99%, Sigma–Aldrich), $AgNO_3$ (99.9%, J.M. Vaz Pereira), $NaBH_4$ (95%, Riedel-de Haën) were used as received without any further purification.

2.2. Synthesis of Au nanospheres

Gold NPs with spherical morphology (hereafter named as nanospheres: NSs) were prepared by reduction of a gold(III) complex using sodium citrate as reducing agent, a method introduced by Turkevitch, Stevenson, and Hillier (1951). Typically 5.64 mL of an aqueous solution of sodium citrate (96.8 mM) was added to 95.5 ml of a $HAuCl_4$ aqueous solution (0.75 mM) at 80 °C, under vigorous stirring, and allowed to react over 1 h. The resulting aqueous Au colloid exhibited a deep red color and showed the characteristic SPR band centered at 520 nm in the optical spectrum (Fig. 1a) (Daniel & Astruc, 2004). The average particle size for Au nanospheres was found to be 10 ± 2 nm as determined by transmission electron microscopy (Fig. 1a). After synthesis the resulting suspension was centrifuged (14,000 rpm for 10 min) and re-dispersed in ultrapure water in order to double and triplicate the original Au NSs concentration.

2.3. Synthesis of Au nanorods

Gold nanorods (NRs) were synthesized by standard protocols based on the seed mediated growth method (Nikoobakht & El-Sayed, 2003). The seed solution was prepared upon the mixture of an aqueous solution of CTAB (5 mL, 0.20 M) with $HAuCl_4$ (5 mL, 0.5 mM). Then 0.6 mL of ice-cold $NaBH_4$ (0.01 M) was added drop wise and vigorously stirred for 2 min. This process resulted in the formation of a brownish yellow solution. The seed solution was kept at 25 °C and used to grow two colloidal samples of Au NRs characterized by a longitudinal optical mode with absorption peaked at 800 nm and 1350 nm, respectively.

Growth of Au NRs (800 nm): An aqueous CTAB solution (5 mL, 0.20 M) was mixed with 0.25 mL of $AgNO_3$ aqueous solution (4 mM) at 25 °C and added to 5 mL of $HAuCl_4$ (1 mM) and this mixture was gently stirred, after which 70 μL of ascorbic acid (78.8 mM) was added. The solution changed from dark yellow to colorless after the addition of ascorbic acid and then 12 μL of the seed solution was added. The resulting solution was kept at 28 ± 1 °C for 1 h with gentle mixing, presenting a pink color at the end.

Growth of Au NRs (1350 nm): A binary surfactant aqueous mixture of CTAB (0.01 g) and BDAC (5 mL, 0.15 M) was prepared by sonication (20 min at 40 °C). This solution was mixed with 200 μL of $AgNO_3$ solution (4 mM), followed by the addition of 5 mL of $HAuCl_4$ (1 mM) upon gentle mixing, after which 70 μL of ascorbic acid (78.8 mM) was added under mild stirring. The final step consisted in the addition of 12 μL of the seed solution. The resulting solution was aged for 7 days at 25 °C.

Prior to nanocomposites preparation, the as prepared Au NRs dispersions (10 mL) were centrifuged (14,000 rpm for 10 min) to remove excess CTAB and the precipitated was re-dispersed in an equal volume of ultrapure water. This procedure was repeated twice. The resulting suspension was re-centrifuged and re-dispersed in ultrapure water in order to double and triplicate the original Au NRs concentration.

The dimensions and aspect ratio of the NRs were estimated from direct measurement using the respective STEM images (Table 1). Two batches of Au NRs with aspect ratios of 3.8 ± 0.8 and 11.8 ± 1.0 whose longitudinal SPR bands were centered respectively at 790 nm and 1350 nm (Fig. 1b and c) have been prepared. Hereafter these NRs are designated by *short* and *long* NRs respectively.

2.4. Preparation of carrageenan nanocomposites

The κ-carrageenan nanocomposites were prepared using Au NSs and NRs of distinct aspect ratios as the nanofillers. The nanocomposites were prepared by blending the nanoparticles with the polymer matrix as follows. A suspension of Au NPs (2.5 mL) was added to 25 mL of a 40 g/L κ-carrageenan solution under magnetic stirring, at 80 °C, followed by the addition of 2.5 mL of KCl 1 M to promote the gelation of κ-carrageenan and stirring. Afterwards 2.5 mL of the composite was transferred to a cylindrical glass vial (Ø 17 mm) and allowed to cool down to room temperature to induce gelation of the composite. Hydrogel composites containing 240, 480 and 720 ppm Au NPs concentration (based on polymer content) were obtained. The gel samples were frozen at −5 °C for 24 h and lyophilized. The final freeze dried discs had approximately 15 mm diameter and 8 mm thickness.

2.5. Materials characterization

Visible–near infrared (Vis–NIR) spectrophotometry: The optical properties of Au NPs and carrageenan/Au nanocomposites were investigated by VIS–NIR analysis of aliquots of the samples. The absorption spectra were recorded using a Jasco V 560 UV–VIS spectrophotometer and a Shimadzu UV–VIS–NIR-3100 instrument.

Electron microscopy: Scanning electron microscopy (SEM) analysis of lyophilized blank hydrogel and carrageenan nanocomposites was performed using a scanning electron microscope Hitachi SU-70 at an accelerating voltage of 15 kV, using carbon sputtered samples. SEM analysis of Au nanorods was performed in transmission mode (STEM) using the same equipment at an accelerating voltage of 30 kV. Transmission electron microscopy (TEM) of Au nanospheres was performed using a transmission electron microscope JEOL 200CX operating at 300 kV. Samples for STEM and TEM analysis were prepared by evaporating dilute suspensions of the nanoparticles on a copper grid coated with an amorphous carbon film.

Differential scanning calorimetry (DSC): The gel–sol transitions of κ-carrageenan hydrogels were determined by DSC using a Shimadzu DSC-50 calorimeter. 30 μL aluminum pans were used with sample masses of *ca.* 25 mg. Hydrogel samples were heated from 25 °C to 80 °C at 2 °C min^{-1}. An empty pan was used as reference.

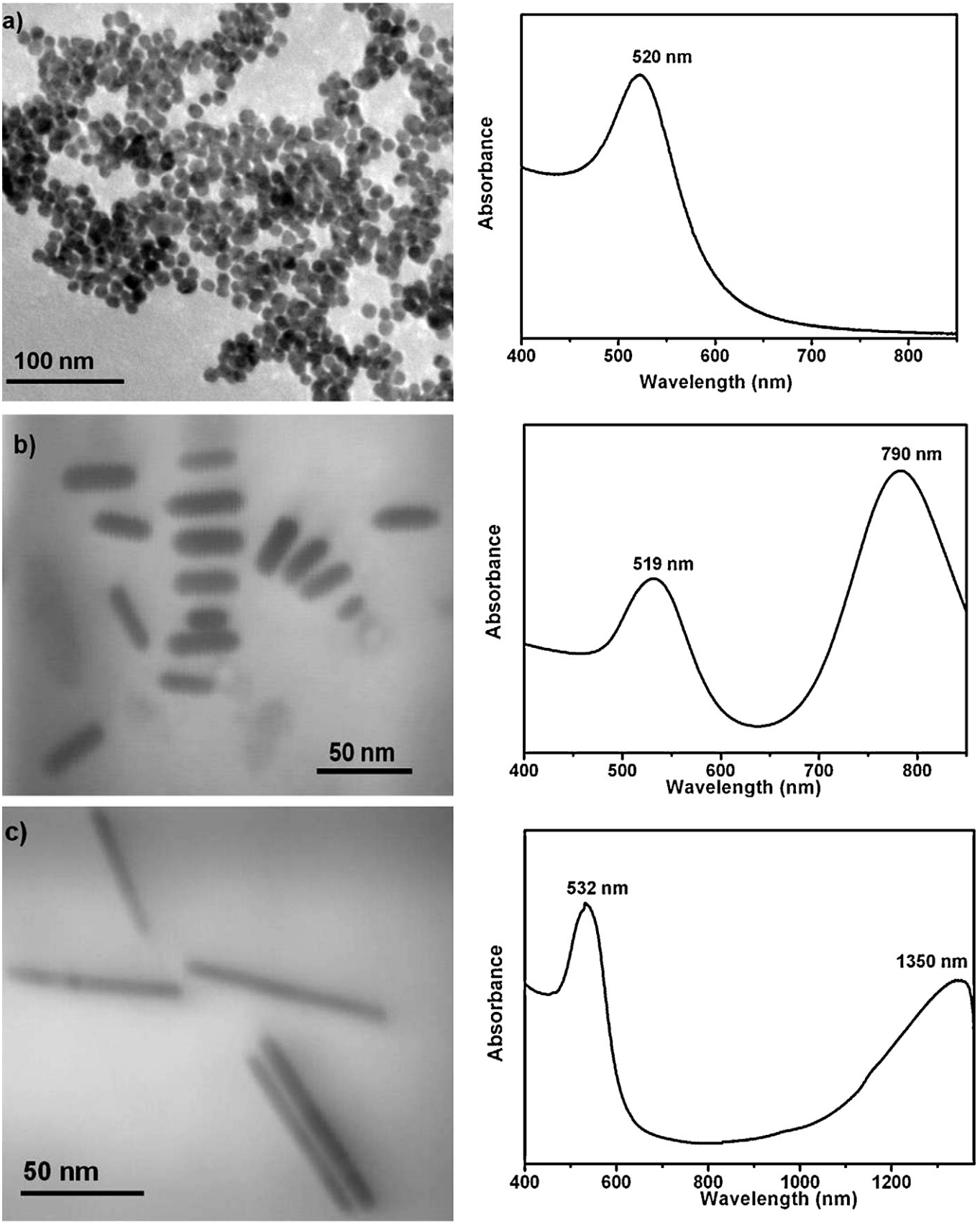

Fig. 1. (a) TEM image of Au nanospheres and STEM images of (b) *short* and (c) *long* Au nanorods and respective Vis–NIR spectra (right side).

Table 1
Average dimensions, aspect ratio and zeta potential (ζ) of Au nanoparticles.

Au NPs	⌀ (nm)	Length (nm)	Thickness (nm)	Aspect ratio	ζ (mV) (pH at 25 °C)
Spheres	10 ± 2	–	–	–	−40.1 ± 0.8 (pH 6.8)
Short rods	–	33 ± 6	9 ± 1	3.8 ± 0.8	43.2 ± 0.3 (pH 5.8)
Long rods	–	77 ± 17	7 ± 1	11.8 ± 1.0	70.7 ± 6.1 (pH 4.2)

Zeta potential measurements: The surface charge of the Au NPs was assessed by zeta potential measurements, using a Zetasizer Nanoseries instrument from Malvern Instruments (UK).

Dynamic mechanical analysis (DMA): The DMA measurements of blank hydrogel and carrageenan nanocomposites were performed on a Tritec 2000 DMA dynamic mechanical analyser (Triton Technology Ltd., UK). The hydrogels were clamped between a parallel-plate compression clamp and an oscillatory deformation with amplitude of 10 μm and a frequency of 1 Hz was applied at various static forces ranging from 0.1 to 0.5 N. The elastic modulus was calculated from extrapolation of experimental data toward zero compression conditions as described elsewhere (Meyvis et al., 2002). DMA measurements were performed in triplicate.

2.6. Swelling studies

The swelling measurements were carried out by immersion of lyophilized hydrogel discs in PBS 0.01 M pH 7.4 at 37 °C. At the required intervals of time, the samples were removed from the solution and wiped with filter paper to remove the excess of water before being weighted. The swelling ratio (Q) was calculated from Eq. (1)

$$Q = \frac{W_s - W_d}{W_d} \quad (1)$$

where W_d and W_s are the weight of the lyophilized and swollen gel, respectively. The equilibrium swelling ratio (Q_{equil}) was determined at the point the hydrated gels achieved a constant weight value. The swelling measurements were performed in triplicate.

2.7. In vitro MB release studies

Methylene blue (MB) was used as a drug model and was loaded during the stage of the preparation of the nanocomposites as described above. MB has been used as a drug model namely because it is a water-soluble dye that allows an immediate visual inspection of the test.

The release experiments were performed in a thermostatic orbital shaker KS 4000I Control from IKA at 37 °C and 120 rpm. A lyophilized disc was introduced in a glass beaker containing 50 mL PBS 0.01 M pH 7.4 and 0.05% (w/v) sodium azide as preserving agent. After predetermined intervals, 1.0 mL of the release medium was drawn and analyzed by UV–Vis spectroscopy (λ = 663 nm) to determine the amount of MB released at each time point and replaced by 1 mL of fresh PBS to maintain the original volume. Prior to UV–Vis analysis the aliquot was diluted into KCl 1 M (dilution ratio 1:6) to ensure that the MB released did not interact with κ-carrageenan (Soedjak, 1994). The effectiveness of the dilution on preventing these interactions was previously confirmed (Daniel-da-Silva et al., 2012). The cumulative released fraction at time t (m_t/m_0) was calculated using Eq. (2)

$$\frac{m_t}{m_0} = \frac{50 \times C_n + \sum_{i=0}^{n-1} C_i}{m_0} \quad (2)$$

where m_t is the cumulative mass of MB released at time t, m_0 is the original mass of MB loaded, C_i is the mass concentration of MB (per ml) of the aliquot, C_n is the mass concentration of MB (per ml) of the aliquot at time t and n is the total number of aliquots extracted until time t. The release experiments were performed in triplicate.

3. Results and discussion

3.1. Optical properties of κ-carrageenan nanocomposites

Gold nanospheres (NSs) and, gold nanorods (NRs) of various aspect ratios, have been synthesized and used as dispersed phases in κ-carrageenan nanocomposites. Nanocomposites were prepared by homogeneous dispersion of Au NPs within a κ-carrageenan aqueous solution, followed by gelation of the mixture upon the addition of K^+ ions that act as chain cross-linkers *via* electrostatic interactions.

The visible spectra of the composite hydrogels (Fig. 2a) show as main absorption features the SPR bands characteristic of the colloids employed in their preparation. In particular, the spectra of the hydrogels containing Au NRs (Fig. 2b and c) display the two absorption bands from the Au NRs used as starting materials. The longitudinal surface plasmon resonance (LSPR) band maximum was blue shifted from 790 nm to 750–770 nm in the composites with *short* NRs, depending on the NRs content, and from 1350 nm to *ca.* 1160 nm in the composites prepared with *long* Au NRs. A small blue shift of the LSPR band (*ca.* 7 nm) of Au NRs in alginate composites as compared to the original Au NR colloid has been previously reported (Mitamura, Imae, Saito, & Takai, 2008). The change in the refractive index of the medium surrounding the Au NRs arising from the presence of polysaccharide molecules as compared to the original hydrosol was advanced as a possible explanation for this slight shift. However the LSPR blue-shift observed here is significantly higher ($\Delta\lambda$ = 20–40 nm and $\Delta\lambda$ = 190 nm for composites with *short* and *long* Au NRs respectively) and may be also indicative of side-by-side assembly of the nanorods in the carrageenan matrix (Sun et al., 2008). Au NRs are stabilized with cationic CTAB which forms a bilayer on the surface of NRs (Nikoobakht & El-Sayed, 2001) and makes their surface positively charged. It is known that the CTAB bilayer is more ordered on the smooth side surface of the NRs than at the curved ends. Moreover the gelation of κ-carrageenan consists in a two step mechanism that involves first the formation of rod shaped carrageenan double helical conformation with an average length of the same order of magnitude than Au NRs (Borgström, Picullel, Viebke, & Talmon, 1996) followed by the parallel aggregation of these helices (Stephen et al., 1995). Thus it may be expected that Au NRs will preferentially align parallel to κ-carrageenan helices due to electrostatic interactions between CTAB and κ-carrageenan molecules. The association of the helices during the gelation of κ-carrageenan will in principle favor the side-by-side assembly of the NRs instead of the end-to-end assembly, which in this case would result in the red-shift of the LSPR maximum band (Sun et al., 2008).

3.2. Microstructure and mechanical properties of hydrogel nanocomposites

With the aim of investigating the effect of Au nanoparticles on the viscoelastic properties of the hydrogel network, the elastic modulus (E') of the hydrogels was assessed by DMA measurements

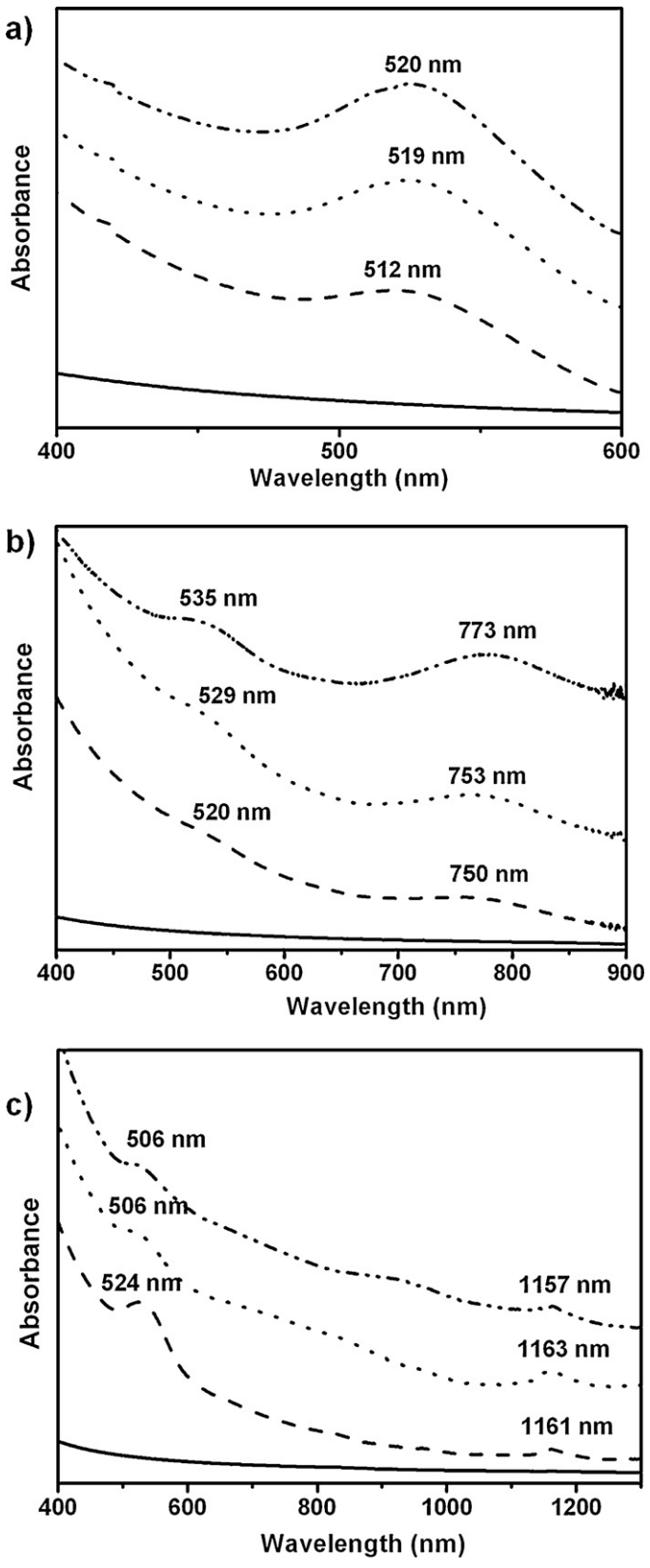

Fig. 2. Absorption spectra of κ-carrageenan/Au hydrogel nanocomposites prepared with (a) Au nanospheres and (b) *short* and (c) *long* Au nanorods. Blank hydrogel (line), 240 ppm Au (- - -); 480 ppm Au (. . .. . .) and 720 ppm Au (. . . - . . .).

Table 2
Elastic modulus (E') of Au/carrageenan nanocomposites calculated from DMA compression mode experiments.

	E' (kPa)		
Blank hydrogel	147.0 ± 11.2		
Au nanocomposites	Au NSs	*Short* NRs	*Long* NRs
240 ppm	191.8 ± 12.1	182.2 ± 33.7	233.7 ± 16.2
480 ppm	216.4 ± 18.3	174.5 ± 32.3	216.8 ± 18.8
720 ppm	209.3 ± 20.1	192.5 ± 29.3	236.7 ± 23.4

(Table 2). Overall the nanocomposites exhibit higher E' values than the blank hydrogel (κ-carrageenan crosslinked with K^+ ions).

The enhancement of the elastic moduli in the composites indicates that the presence of Au NPs, either nanospheres or nanorods, promotes the formation of stronger κ-carrageenan hydrogels. However, and as discussed below, we propose that this effect originates in distinct types of interactions depending on the surface chemistry of the fillers employed. As previously mentioned, the formation of κ-carrageenan gel network involves the side-by-side aggregation of helical conformations of polymer chains and is promoted by cations such as K^+ ions (Stephen et al., 1995). Au NSs are colloidal stable because surface chemisorbed citrate ions imparts a net negative charge to the particles causing electrostatic repulsion. This was further confirmed by zeta potential measurements (−40.1 ± 0.8 mV, Table 1) performed on the aqueous Au colloids. The repulsive electrostatic interactions between the negatively charged Au nanospheres and the sulphate groups of κ-carrageenan would in principle disfavor the association of carrageenan chains and thus originate weaker gels. Since the opposite effect was observed, a possible explanation may rely on the adsorption of K^+ ions at the negatively charged surface of the Au NSs. This would result in an increase of K^+ counterions around Au NSs due to electrostatic interactions, which are surrounded by carrageenan molecules, and promote more extensive biopolymer helical aggregation, thus resulting in the formation of stronger κ-carrageenan gels in the presence of Au NSs, as observed. A similar mechanism has been proposed to explain the formation of stronger κ-carrageenan gels in the presence of negatively surface charged Fe_3O_4 nanoparticles (Daniel-da-Silva et al., 2008).

The zeta potential of the Au NRs was found to be 43.2 ± 0.3 mV and 70.7 ± 6.1 mV (Table 1) for low and high aspect ratios respectively, consistent with the presence of a bilayer of positively charged ammonium surfactant molecules (CTAB) at the surface of the nanorods (Nikoobakht & El-Sayed, 2001). Conversely to the Au NSs discussed above, the NRs have positive surface charge and thus a possible explanation for the increase of E' in these composites relies on the aggregation of carrageenan chains due to electrostatic interactions between the sulfate groups of κ-carrageenan and the positively charged CTAB molecules. This is in agreement with previous findings reporting the shrinkage of κ-carrageenan micro- and nanospheres in the presence of CTAB due to electrostatic interactions between CTAB and κ-carrageenan (Daniel-da-Silva et al., 2011; Ellis, Keppeler, & Jacquier, 2009). BDAC surfactant molecules that exist at the surface of the *long* NRs were found to promote a similar effect on κ-carrageenan spheres (Ellis et al., 2009). These electrostatic interactions and the hydrophobic alkyl chain of CTAB and BDAC force the carrageenan strands close together (Ellis et al., 2009), hence leading to denser polymeric networks whose E' values are higher than those of blank hydrogels. The incorporation of *long* Au NRs resulted in hydrogels with the highest E' values most likely due to differences in the surface charge of these fillers. *Long* Au NRs, because they are more positively charged than *short* NRs may originate stronger electrostatic interactions with carrageenan

molecules and thus leading to denser polymer network than in hydrogels containing *short* NRs.

Further insight into the structure of the gel network was obtained by DSC measurements. The DSC thermograms of κ-carrageenan hydrogel and nanocomposites (Fig. 3) show a broad endothermic peak that corresponds to the melting (gel-to-sol transition) of the hydrogel. The values of the melting temperature (T_m), defined here as the temperature of the main peak, are included in Table S1 of supplementary data. For the blank κ-carrageenan hydrogel the peak is centered at about 47 °C. As a consequence of incorporating Au NPs in the hydrogel, the peak shifted to higher temperatures. Adding Au NPs also originates an increase of the area of the endothermic peak, which is directly related to the enthalpy of the melting process (ΔH_m). The values of ΔH_m are included in Table S1 of supplementary material.

The mechanism of melting of κ-carrageenan hydrogels is known to involve the breaking up of aggregates of double helical conformations which act as physical junctions in the gel (Stephen et al., 1995). The increase of T_m and ΔH_m might be explained by the reinforcement of the gel structure by the Au NPs, delaying the gel collapse. These results seem to confirm that the Au NPs promote the reinforcement of the κ-carrageenan gels structure, in agreement with the enhancement of the elastic moduli observed by DMA and as discussed above. From the analysis of the DSC thermograms (Fig. 3 and Table S1) arises that, for equivalent Au content, the hydrogels containing Au NSs undergo melting at higher temperature than those containing anisotropic Au NRs. Also, it may be observed that the thermograms of the hydrogels containing Au NSs show one main broad peak. In opposition, the thermograms of the hydrogels containing Au NRs show several subpeaks at temperatures lower and higher than the main peak. These observations are in line with previous works (Daniel-da-Silva et al., 2011; Iijima, Hatakeyama, Takahashi, & Hatakeyama, 2007) and suggest that carrageenan helices and aggregates having various sizes and thus undergoing melting at different temperatures, might be present in the hydrogels containing Au NRs rendering the gel network less homogeneous than in κ-carrageenan alone and the composites with Au NSs.

The SEM images of lyophilized hydrogels are shown in Fig. 4. These images show that the structural changes induced in the gel upon the addition of Au NPs are realized at a microscopic level. The blank hydrogel shows a continuous structure comprising polymer flakes and irregular pores with high interconnectivity (Fig. 4a). The polymer flakes become larger upon the addition of Au NSs (Fig. 4b) which is consistent with an extended association of carrageenan helices promoted by these NPs. Hydrogels containing Au NRs show polymer flakes having variable dimensions (Fig. 4c and d). These images are consistent with DSC results and corroborate that the introduction of anisotropic Au NRs originates a less homogeneous microstructure with helices aggregates of various sizes. This effect is illustrated in Fig. 5. Blank hydrogel (Fig. 5a) is composed by smaller helical aggregates. When spherical Au NPs are added as dispersed phase (Fig. 5b), the carrageenan molecules are able to organize themselves evenly around the Au NPs, these promoting the formation of larger and uniformly sized aggregates and thus resulting in a more homogeneous gel microstructure than in the Au NRs filled hydrogel (Fig. 5c).

3.3. Swelling properties

The equilibrium swelling ratio (Q_{equil}) of the blank κ-carrageenan hydrogel was 21.8 ± 1.8. Depending on the aspect ratio and content of the Au NPs, hydrogel composites achieved Q_{equil} equivalent to or higher than pure κ-carrageenan (Fig. 6).

As previously demonstrated by DSC and DMA measurements, the composites have a reinforced polymeric structure as compared

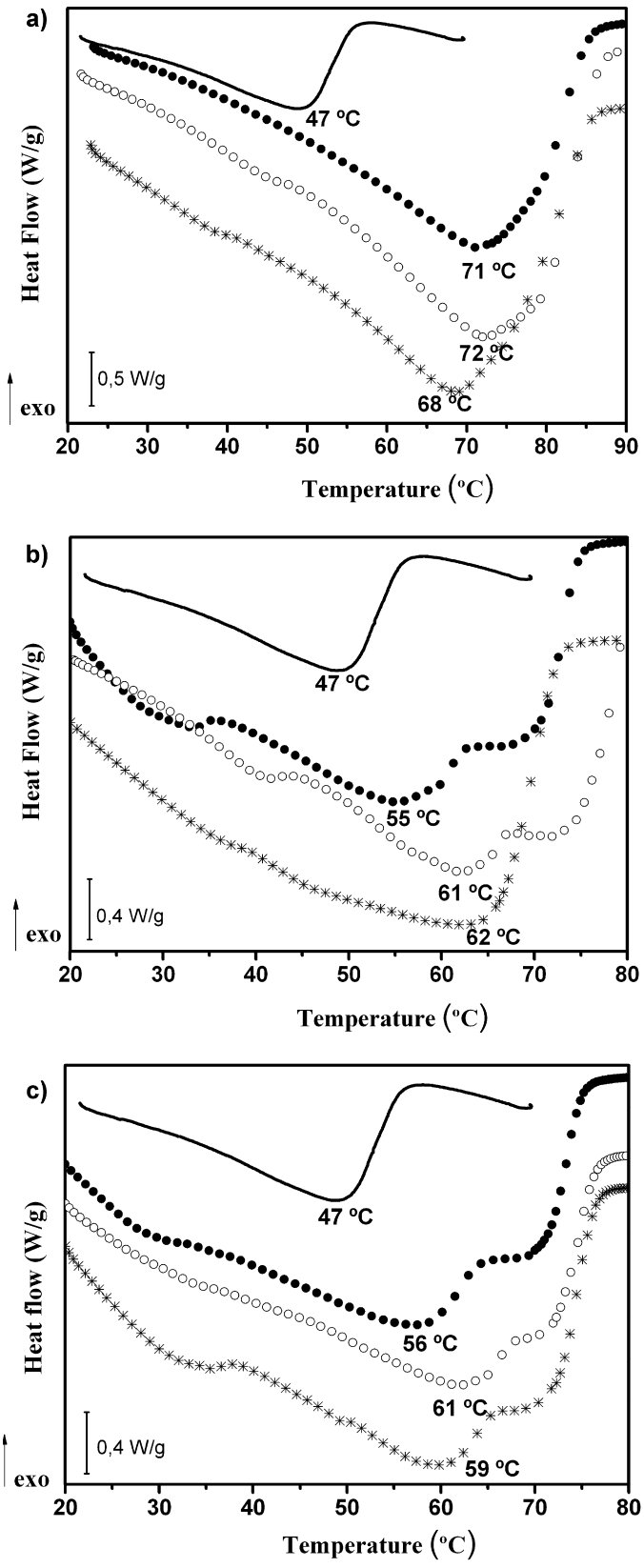

Fig. 3. DSC thermograms of κ-carrageenan nanocomposites prepared with (a) Au nanospheres and (b) *short* and (c) *long* Au nanorods. κ-Carrageenan alone (line) and composites with 240 ppm of Au NPs (full circle), 480 ppm (open circle) and 720 ppm (star).

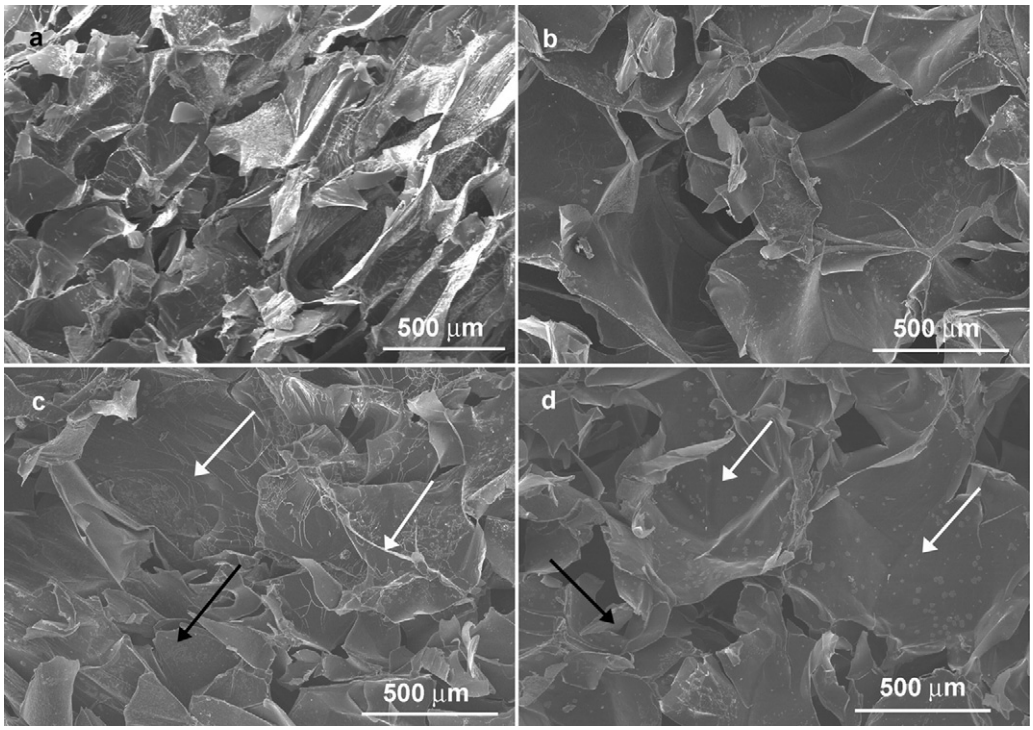

Fig. 4. SEM micrographs of lyophilized (a) blank hydrogel and nanocomposites containing (b) Au NSs, (c) *short* Au NRs and (d) *long* Au NRs at a concentration of 720 ppm (white and black arrows indicate polymer flakes with large and small dimensions, respectively, in the hydrogels containing Au NRs).

to the neat hydrogel, thereby lower Q_{equil} would be expected on the basis of gel strength values. However, our recent work has shown that the swelling of κ-carrageenan hydrogels containing Fe_3O_4 NPs depends on the balance between the viscoelastic properties of the polymeric network and the charge of the nanocomposites, both being affected by the incorporation of the nanofillers (Daniel-da-Silva et al., 2012). A similar effect might be expected upon the addition of Au NPs and indeed the composite formulations investigated here have exhibited in general Q_{equil} higher than the corresponding value for the blank hydrogel (Fig. 6). For example, the hydrogels filled with Au NSs exhibited higher Q_{equil} than κ-carrageenan, despite having higher E' than the blank hydrogel. The increase of Q_{equil} was more pronounced in the composites containing 240 ppm NSs and can be attributed to the introduction of charged Au NPs in the hydrogel. The immobilization of surface charged Au NPs within ionic hydrogels such as κ-carrageenan results in an afflux of water to balance the osmotic pressure build-up, which causes the hydrogel to swell. Further incorporation of Au NSs results in an additional strengthening of the polymer network, as observed by the increase of E' of the hydrogels, (Table 2) which will exerts the opposite effect and restrict the swelling of the hydrogels. Despite the high surface charge of the *long* Au NRs, the corresponding composites swelled less than those filled with NSs and swells similarly to the blank hydrogel, a behavior that can be explained by the enhanced viscoelastic properties of these composites (Table 2).

3.4. MB release studies

Hydrogel nanocomposites with Au NPs content of 240 ppm were selected for *in vitro* MB release studies. The amount of released MB was monitored by measuring the absorbance of the release medium at 663 nm, *i.e.* at the wavelength of maximum absorbance for MB. To limit the interaction of MB molecules with the κ-carrageenan chains, KCl was added to the aliquots prior to UV/Vis analysis (Daniel-da-Silva et al., 2012). Fig. 7 displays the release patterns of MB in PBS from κ-carrageenan alone and composite discs. The release profiles from the blank hydrogel and the composites containing *short* NRs are similar. However, the latter shows a MB release slightly faster in the first 2 h, most probably as consequence of the electrostatic repulsions between the cationic surfactants at the surface of the Au NRs and the MB molecules. This effect seems more pronounced for composites containing *long* NRs. After 5 h the MB release from the composites with *long* Au NRs slows down significantly, which could be attributed to the enhanced viscoelastic properties of these composites. The release profile from the composites containing Au NSs shows more marked differences. At an initial stage, the release is slower than in the blank hydrogel and then progresses to a more rapid release at later stage before leveling, thus resulting in a sigmoidal profile. The concave-upward profile is most likely due to the interaction between MB and Au nanospheres. Methylene blue interacts strongly with gold nanoparticles most probably by surface chemisorption *via* sulphur atoms (Narband et al., 2009). Thus, a possible explanation is that the diffusion of MB molecules to the release medium is limited due to chemisorption of MB onto Au NSs located within the polymer matrix. For example, the decrease of MB release from polysiloxane polymers due to the incorporation of gold NSs has been reported (Perni et al., 2009). This sorption effect is not expected to occur onto Au NRs due to the presence of the cationic surfactants at the surface of these particles. The fast release of MB at later stages can be related to the high equilibrium swelling observed for composites containing Au NSs (Fig. 7). This is in agreement with our previous work dealing with the swelling and release properties of κ-carrageenan/Fe_3O_4 hydrogel nanocomposites (Daniel-da-Silva et al., 2012). In this work it was observed a sigmoidal MB release profile for hydrogels showing high values of equilibrium swelling ratio, hence indicating that the transport of the MB from the matrix to the surrounding medium is facilitated in the swollen matrix.

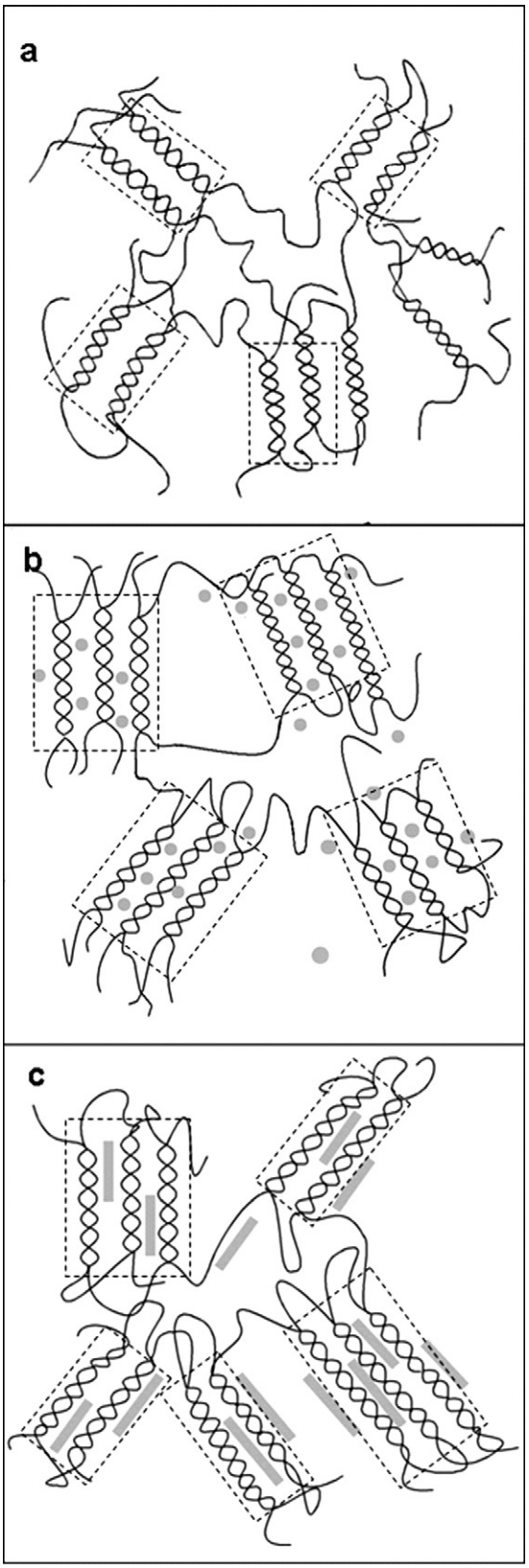

Fig. 5. Schematic illustration of the κ-carrageenan gel network of (a) blank hydrogel and nanocomposites with (b) Au NSs and (c) Au NRs (dashed lines delimit aggregates).

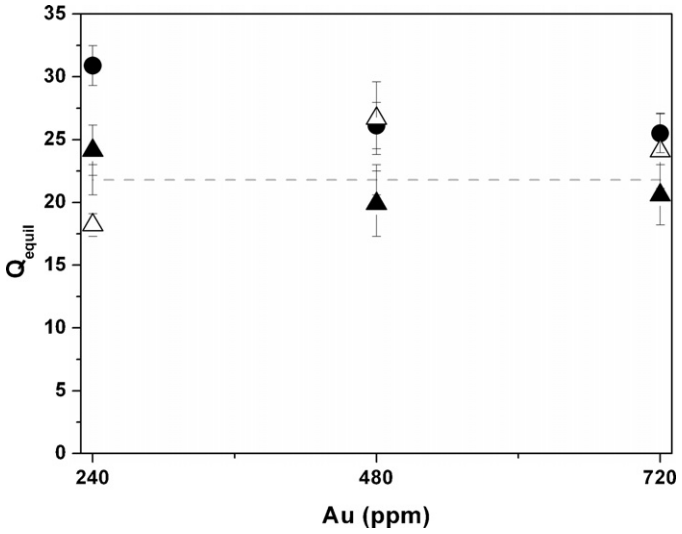

Fig. 6. Swelling ratio at equillibrium (Q_{equil}) of unfilled κ-carrageenan hydrogel and Au nanocomposites. Blank hydrogel (dashed line), nanospheres (•), *short* nanorods (△) and *long* nanorods (▲).

With the aim of gaining insight into the release mechanism, the experimental release data were fitted to the Ritger–Peppas model for $(m_t/m_\infty) \leq 0.6$, a semi-empirical power law described by Eq. (3)

$$\frac{m_t}{m_\infty} = kt^n \tag{3}$$

where m_t is the cumulative amount of drug released at time t, m_∞ is the cumulative amount of drug released at infinite time, k is a constant incorporating structural and geometric characteristics of the carrier and n is the release exponent indicative of the mechanism of drug release that depends also of the geometry of the carrier (Ritger & Peppas, 1987). For a radial diffusion from a cylindrical carrier such as those used here, n takes the value of 0.45 when the release is driven by pure drug diffusion (Fick's law). When $n = 0.89$ the drug release rate is constant in time and corresponds to zero-order release kinetics, also termed as case-II transport and the drug release follows a polymer chain relaxation mechanism. The constant k and the exponent n estimated for each system as well as the corresponding coefficient of determination (R^2) are listed in

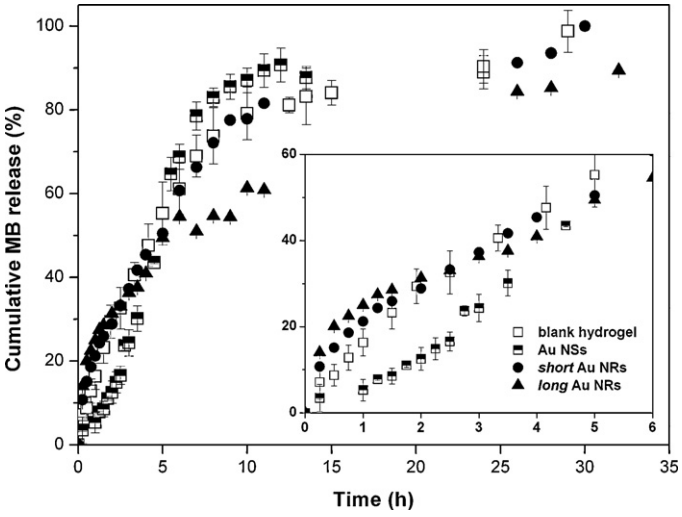

Fig. 7. *In vitro* MB release profiles from the blank hydrogel and hydrogel nanocomposites containing Au nanoparticles at a concentration of 240 ppm.

Table 3
Parameters k and n, as estimated from the application of the Ritger–Peppas model to the MB release data, and coefficient of determination (R^2).

Sample		$k \times 10^3$ [min^{-n}]	n	R^2
Blank hydrogel		8.32 ± 0.92	0.74 ± 0.02	0.997
Au composites	NSs	0.13 ± 0.04	1.45 ± 0.06	0.991
240 ppm	*Short* NRs	19.86 ± 2.19	0.57 ± 0.02	0.990
	Long NRs	52.61 ± 1.79	0.38 ± 0.01	0.997

Table 3. The data appear correctly fitted by this model as R^2 was greater than 0.99.

The n value found for the release of MB from blank hydrogel was 0.74, which suggests anomalous release. This indicates that the polymer relaxation time is comparable to the diffusion time (Fu & Kao, 2010). The addition of Au NSs increases n to values higher than 1, which suggests super case-II transport and corresponds to a mechanism controlled by erosion and polymer relaxation. The MB release from specific compositions of magnetic κ-carrageenan nanocomposites was found to follow a similar mechanism (Daniel-da-Silva et al., 2012). These composites had in common with the Au NSs composites here investigated the ability to uptake high amounts of water, hence showing high values of $Q_{equil.}$ The high water availability in the polymer matrix most probably leads to an increased plasticization and polymer erosion, which is in agreement with previous observations on other polymer systems showing the same kind of release mechanism (Charoenthai, Kleinebudde, & Puttipipatkhachorn, 2007; Soo et al., 2008; Sriamornsak, Thirawong, & Korkerd, 2007).

The incorporation of Au NRs decreases the exponent from 0.74 in the blank hydrogel to 0.54 and to 0.38 for composites containing *short* and *long* NRs respectively. Both values are close to 0.45 which indicates a change in the release mechanism to diffusion-controlled. These results show that, in spite of the high elastic moduli of the hydrogels containing Au NRs when compared to pure κ-carrageenan, the release of MB molecules is not limited by the relaxation of the polymer chains. Hence, the incorporation of Au NRs seems to slow down the diffusion rate of the MB molecules. This is most likely due to the influence of the Au NRs on the tortuosity of the κ-carrageenan matrix. The incorporation of Au NRs originates a polymer network more heterogeneous than in the original hydrogel as found out by DSC (Fig. 3) and confirmed by microscopy analysis (Fig. 4). This could lead to changes in the tortuosity, a parameter which accounts for contribution of the average pore size, the pore size distribution and the pore interconnectivity of the hydrogel and that is inversely related to the diffusion coefficient (Hoffman, 2002). An increased tortuosity of the carrageenan network due to twisting or distortion of pores would result in smaller MB diffusion rates and could lead to a diffusion controlled mechanism. This is in agreement with previous findings reporting the reduction of the release rate (Thrimawithana, Young, & Alany, 2011) and diffusion coefficients (Walther, Lorén, Nydén, & Hermansson, 2006) of molecules incorporated in κ-carrageenan gels with increased tortuosity (arising from small pore size) of the hydrogel microstructure.

4. Conclusions

The effect of incorporating spherical and rod-shaped gold nanoparticles in the microstructure and thermomechanical properties of κ-carrageenan hydrogels and in the release kinetics and mechanism of methylene blue (MB) from κ-carrageenan nanocomposites was investigated. Hydrogel nanocomposites showed enhanced viscoelastic properties as compared to neat κ-carrageenan, when using either Au NSs or Au NRs. A mechanism is proposed for the reinforcement effect that takes into account the distinct surface chemistry of gold nanospheres and gold nanorods. The anisotropy of the nanofillers was found to affect the aggregation of κ-carrageenan helices rendering the microstructure of the hydrogel network less homogeneous.

For equivalent Au NPs content, the MB release kinetics depended on the nature of the Au NPs used as dispersed phase. While the release of MB from κ-carrageenan hydrogels followed an anomalous transport, it tended to be controlled by polymer relaxation and erosion if spherical Au NPs were incorporated and diffusion controlled if rod-shaped Au NPs were incorporated as dispersed phase. Considering that the introduction of both Au NSs and NRs originates stronger hydrogels it would be expected that MB release followed a polymer relaxation mechanism regardless the shape of the Au NPs. It is suggested that the heterogeneous gel microstructure arising from the incorporation of anisotropic Au NPs increases the tortuosity of MB path, rendering the MB release diffusion controlled.

These findings can be further explored for adjusting the drug release from carriers based on other biopolymers with gelation schemes similar to κ-carrageenan (*e.g.* agarose, gellan gum) and have broad implications in the design of novel biomaterials for controlled drug release.

Acknowledgements

The authors acknowledge FCT (ERA-Eula/0003/2009), Pest-C/CTM/LA0011/2011, FSE and POPH for funding. We thank the RNME (National Electronic Microscopy Network) for SEM and TEM images and the National Program for Scientific Equipment Renewal (REED/515/CTM/2005) for DMA measurements. The authors are very grateful to Dr. A.V. Girão, MSc. M.C. Azevedo and MSc. S. Magina for technical support.

Appendix A. Supplementary data

Supplementary data associated with this article can be found, in the online version, at doi:10.1016/j.carbpol.2012.08.004.

References

Bhattarai, N., Gunn, J., & Zhang, M. (2010). Chitosan-based hydrogels for controlled, localized drug delivery. *Advanced Drug Delivery Reviews*, *62*, 83–99.
Borgström, J., Picullel, L., Viebke, C., & Talmon, Y. (1996). On the structure of aggregated kappa-carrageenan helices. A study by cryo-TEM, optical rotation and viscometry. *International Journal of Biological Macromolecules*, *18*, 223–229.
Charoenthai, N., Kleinebudde, P., & Puttipipatkhachorn, S. (2007). Use of chitosan-alginate as alternative pelletization aid to microcrystalline cellulose in extrusion/spheronization. *Journal of Pharmaceutical Sciences*, *96*, 2469–2484.
Choi, W. I., Kim, J. K., Kang, C., Byeon, C. C., Kim, Y. H., & Taet, G. (2011). Tumor regression in vivo by photothermal therapy based on gold-nanorod-loaded, functional nanocarriers. *ACS Nano*, *5*, 1995–2003.
Daniel, M. C., & Astruc, D. (2004). Gold nanoparticles: Assembly, supramolecular chemistry, quantum-size-related properties, and applications toward biology, catalysis, and nanotechnology. *Chemical Reviews*, *104*, 293–346.
Daniel-da-Silva, A. L., Ferreira, L., Gil, A. M., & Trindade, T. (2011). Synthesis and swelling behavior of temperature responsive κ-carrageenan nanogels. *Journal of Colloid and Interface Science*, *355*, 512–517.
Daniel-da-Silva, A. L., Lóio, R., Lopes-da-Silva, J. A., Trindade, T., Goodfellow, B. J., & Gil, A. M. (2008). Effects of magnetite nanoparticles on the thermorheological properties of carrageenan hydrogels. *Journal of Colloid and Interface Science*, *324*, 205–211.
Daniel-da-Silva, A. L., Moreira, J., Neto, R., Estrada, A. C., Gil, A. M., & Trindade, T. (2012). Impact of magnetic nanofillers in the swelling and release properties of κ-carrageenan hydrogel nanocomposites. *Carbohydrate Polymers*, *87*, 328–335.
Daniel-da-Silva, A. L., Trindade, T., Goodfellow, B. J., Costa, B. F. O., Correia, R. N., & Gil, A. M. (2007). In situ synthesis of magnetite nanoparticles in carrageenan gels. *Biomacromolecules*, *8*, 2350–2357.
Du, Y., Luo, X.-L., Xu, J.-J., & Chen, H.-Y. (2007). A simple method to fabricate a chitosan–gold nanoparticles film and its application in glucose biosensor. *Bioelectrochemistry*, *70*, 342–347.
Ellis, A., Keppeler, S., & Jacquier, J. C. (2009). Responsiveness of κ-carrageenan microgels to cationic surfactants and neutral salts. *Carbohydrate Polymers*, *78*, 384–388.

Fu, Y., & Kao, W. J. (2010). Drug release kinetics and transport mechanisms of non-degradable and degradable polymeric delivery systems. *Expert Opinion on Drug Delivery*, *7*, 429–444.

Guo, R., Zhang, L., Qian, H., Li, R., Jiang, X., & Liu, B. (2010). Multifunctional nanocarriers for cell imaging, drug delivery, and near-IR photothermal therapy. *Langmuir*, *26*, 5428–5434.

Hoffman, A. S. (2002). Hydrogels for biomedical applications. *Advanced Drug Delivery Reviews*, *54*, 3–12.

Iijima, M., Hatakeyama, T., Takahashi, M., & Hatakeyama, H. (2007). Effect of thermal history on kappa-carrageenan hydrogelation by differential scanning calorimetry. *Thermochimica Acta*, *452*, 53–58.

Jain, A., Gupta, Y., & Jain, S. K. (2007). Perspectives of biodegradable natural polysaccharides for site specific drug delivery to the colon. *Journal of Pharmacy and Pharmaceutical Sciences*, *10*, 86–128.

Keppeler, S., Ellis, A., & Jacquier, J. C. (2009). Cross-linked carrageenan beads for controlled release delivery systems. *Carbohydrate Polymers*, *78*, 973–977.

Leong, K. H., Chung, L. Y., Noordin, M. I., Mohamad, K., Nishikawa, M., Onuki, Y., Morishitab, M., & Takayamabet, K. (2011). Carboxymethylation of kappa-carrageenan for intestinal-targeted delivery of bioactive macromolecules. *Carbohydrate Polymers*, *83*, 1507–1515.

Lim, S. Y., Lee, J. S., & Park, C. B. (2010). In situ growth of gold nanoparticles by enzymatic glucose oxidation within alginate gel matrix. *Biotechnology and Bioengineering*, *105*, 210–214.

Matteini, P., Ratto, F., Rossi, F., Centi, S., Dei, L., & Pini, R. (2010). Chitosan films doped with gold nanorods as laser-activatable hybrid bioadhesives. *Advanced Materials*, *22*, 4313–4316.

Meyvis, T. K. L., Stubbe, B. G., VanSteenbergen, M. J., Hennink, W. E., DeSmedt, S. C., & Demeester, J. (2002). A comparison between the use of dynamic mechanical analysis and oscillatory shear rheometry for the characterisation of hydrogels. *International Journal of Pharmaceutics*, *244*, 163–168.

Mitamura, K., Imae, T., Saito, N., & Takai, O. (2008). Fabrication and structure of alginate gel incorporating gold nanorods. *Journal of Physical Chemistry C*, *112*, 416–422.

Narband, N., Uppal, M., Dunnill, C. W., Hyett, G., Wilson, M., & Parkin, I. P. (2009). The interaction between gold nanoparticles and cationic and anionic dyes: Enhanced UV–visible absorption. *Physical Chemistry Chemical Physics*, *11*, 10513–10518.

Nikoobakht, B., & El-Sayed, M. A. (2001). Evidence for bilayer assembly of cationic surfactants on the surface of gold nanorods. *Langmuir*, *17*, 6368–6374.

Nikoobakht, B., & El-Sayed, M. A. (2003). Preparation and growth mechanism of gold nanorods (NRs) using seed-mediated growth method. *Chemistry of Materials*, *15*, 1957–1962.

Perni, S., Piccirillo, C., Pratten, J., Prokopovich, P., Chrzanowski, W., Parkin, I. P., & Wilson, M. (2009). The antimicrobial properties of light-activated polymers containing methylene blue and gold nanoparticles. *Biomaterials*, *30*, 89–93.

Ritger, P. L., & Peppas, N. A. (1987). A simple equation for description of solute release II. Fickian and anomalous release from swellable devices. *Journal of Controlled Release*, *5*, 37–42.

Santo, V. E., Frias, A. M., Carida, M., Cancedda, R., Gomes, M. E., Mano, J. F., & Reis, R. L. (2009). Carrageenan-based hydrogels for the controlled delivery of PDGF-BB in bone tissue engineering applications. *Biomacromolecules*, *10*, 1392–1401.

Satarkar, N. S., Biswal, D., & Hilt, J. Z. (2010). Hydrogel nanocomposites: A review of applications as remote controlled biomaterials. *Soft Matter*, *6*, 2364–2371.

Sharma, V., Park, K., & Srinivasarao, M. (2009). Colloidal dispersion of gold nanorods: Historical background, optical properties, seed-mediated synthesis, shape separation and self-assembly. *Materials Science and Engineering Reports*, *65*, 1–38.

Soedjak, H. S. (1994). Colorimetric determination of carrageenans and other anionic hydrocolloids with methylene blue. *Analytical Chemistry*, *66*, 4514–4518.

Soo, P. L., Cho, J., Grant, J., Ho, E., Piquette-Miller, M., & Allen, C. (2008). Drug release mechanism of paclitaxel from a chitosan–lipid implant system: Effect of swelling, degradation and morphology. *European Journal of Pharmaceutics and Biopharmaceutics*, *69*, 149–157.

Sriamornsak, P., Thirawong, N., & Korkerd, K. (2007). Swelling, erosion and release behavior of alginate-based matrix tablets. *European Journal of Pharmaceutics and Biopharmaceutics*, *66*, 435–450.

Stephen, A. M., Philips, G. O., & Williams, P. A. (1995). *Food polysaccharides and their applications*. New York: Marcel Dekker., pp. 205–217.

Stone, J., Jackson, S., & Wright, D. (2011). Biological applications of gold nanorods. *WIREs Nanomedicine and Nanobiotechnology*, *3*, 100–109.

Sun, Z., Ni, W., Yang, Z., Kou, X., Li, L., & Wang, J. (2008). pH-controlled reversible assembly and disassembly of gold nanorods. *Small*, *4*, 1287–1292.

Thrimawithana, T. R., Young, S., & Alany, R. G. (2011). Effect of cations on the microstructure and in vitro drug release of κ- and ι-carrageenan liquid and semi-solid aqueous dispersions. *Journal of Pharmacy and Pharmacology*, *63*, 11–18.

Timko, B. P., Dvir, T., & Kohane, D. S. (2010). Remotely triggerable drug delivery systems. *Advanced Materials*, *22*, 4925–4943.

Trindade, T., & Daniel-da-Silva, A. L. (2011). *Nanocomposite particles for bio-applications: Materials and bio-interfaces*. Singapore: Pan Stanford Publishing Pte. Ltd.

Turkevitch, J., Stevenson, P. C., & Hillier, J. (1951). A study of the nucleation and growth processes in the synthesis of colloidal gold. *Discussions of the Faraday Society*, *11*, 55–75.

Walther, B., Lorén, N., Nydén, M., & Hermansson, A.-M. (2006). Influence of κ-carrageenan gel structures on the diffusion of probe molecules determined by transmission electron microscopy and NMR diffusometry. *Langmuir*, *22*, 8221–8228.